

Mitigation of Tensile Weld Stresses in Alloy 22 Using Laser Peening

H.-L. Chen, et. al

November 27, 2002

U.S. Department of Energy

Lawrence
Livermore
National
Laboratory

DISCLAIMER

This document was prepared as an account of work sponsored by an agency of the United States Government. Neither the United States Government nor the University of California nor any of their employees, makes any warranty, express or implied, or assumes any legal liability or responsibility for the accuracy, completeness, or usefulness of any information, apparatus, product, or process disclosed, or represents that its use would not infringe privately owned rights. Reference herein to any specific commercial product, process, or service by trade name, trademark, manufacturer, or otherwise, does not necessarily constitute or imply its endorsement, recommendation, or favoring by the United States Government or the University of California. The views and opinions of authors expressed herein do not necessarily state or reflect those of the United States Government or the University of California, and shall not be used for advertising or product endorsement purposes.

This work was performed under the auspices of the U. S. Department of Energy by the University of California, Lawrence Livermore National Laboratory under Contract No. W-7405-Eng-48.

This report has been reproduced directly from the best available copy.

Available electronically at <http://www.doc.gov/bridge>

Available for a processing fee to U.S. Department of Energy
And its contractors in paper from
U.S. Department of Energy
Office of Scientific and Technical Information
P.O. Box 62
Oak Ridge, TN 37831-0062
Telephone: (865) 576-8401
Facsimile: (865) 576-5728
E-mail: reports@adonis.osti.gov

Available for the sale to the public from
U.S. Department of Commerce
National Technical Information Service
5285 Port Royal Road
Springfield, VA 22161
Telephone: (800) 553-6847
Facsimile: (703) 605-6900
E-mail: orders@ntis.fedworld.gov
Online ordering: <http://www.ntis.gov/ordering.htm>

OR

Lawrence Livermore National Laboratory
Technical Information Department's Digital Library
<http://www.llnl.gov/tid/Library.html>

Mitigation of Tensile Weld Stresses in Alloy 22 Using Laser Peening

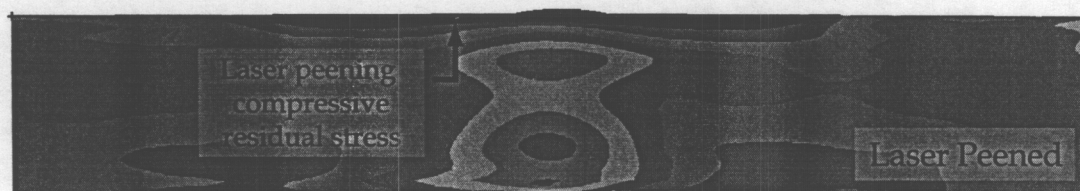
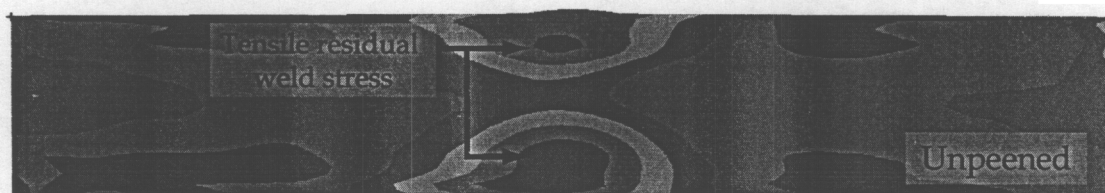
Interim Report
November 2002

Hao-Lin Chen
Kenneth J. Evans
Lloyd A. Hackel
Jon E. Rankin
Robert M. Yamamoto

*Lawrence Livermore
National Laboratory*

Anne G. Demma
Adrian T. Dewald
Matthew J. Lee
Michael R. Hill

*University of California,
Davis*



Executive Summary

Ensuring the structural integrity of the waste package (WP) closure weld is a major development task in support of the Yucca Mountain Project (YMP). A series of tests were performed at the Lawrence Livermore National Laboratory (LLNL) in cooperation with the University of California, Davis (UC Davis) on Alloy 22 base metal and weld coupons to characterize the effects the Laser Peening (LP) process has on these material configurations.

The test results show that the laser peening process produces peak values of compressive residual stress of several hundred MPa. Residual stress remains compressive to a depth on the order of 5 mm into Alloy 22 parent and weld material. This will significantly improve the material's resistance to stress corrosion cracking. In addition, accelerated corrosion tests show that an Alloy 22 laser peened surface corrodes at a much-reduced rate as compared to an untreated surface.

The development at LLNL of very high-energy pulsed laser systems has allowed the laser peening process to advance from a laboratory tool to a true production equipment status. An initial engineering study has concluded that this laser peening process can be readily deployed in a remote, radioactive environment and be fully compatible with the YMP surface facilities, which includes reliability and operational maintainability requirements. Laser peening times of several hours per disposal container (DC) can be maintained, commensurate with the operational timeline for the entire closure system.

The Laser Peening System is an industrially viable process. Commercial jet engine components have undergone the laser peening process to increase their operational lifetime several fold. A production system built jointly by LLNL and their industrial partner, Metal Improvement Company (MIC), was put into commercial service in May 2002. This production process has received Federal and Canadian Aviation Administration (FAA and CAA) certification as commercial aircraft utilizing the laser peening process are in use today. Over \$120 million in commercial aircraft parts have been treated utilizing laser peening, affecting \$6 billion in aircraft and saving \$30 million per month in aircraft maintenance costs.

As a consequence of this work, a new method for measuring the cross-sectional residual stresses in the welded Alloy 22 plates was used. The contour method was employed which provides a full two-dimensional cross-sectional map of the residual stress. In addition, the slitting method of measuring residual stresses was also utilized to provide complementary understanding and result verification. Details on both of these stress measurement techniques are included in this report.

Introduction

The goal of the Yucca Mountain Project (YMP) is safe permanent disposal of high-level nuclear waste. One of the many technical challenges to this plan is the design of the Engineered Barrier System (EBS) including the waste package that will contain the radioactive waste. One potential failure mode of the waste package is stress corrosion cracking (SCC), which occurs when three criteria simultaneously exist. These criteria are a potentially corrosive environment, a material susceptible to SCC, and the presence of tensile residual stresses at the surface of the material. While many design decisions have been made to attempt to minimize the occurrence of the first two conditions, it is necessary to control the third condition, the presence of tensile residual stresses. These stresses occur as a result of a variety of manufacturing techniques, including welding. While most of the residual stresses due to the welding of the waste package can be mitigated through solution heat-treating, the final closure weld, which occurs after the radioactive waste has been placed in the waste package, must be treated to eliminate the presence of tensile residual stress near the surface.

Laser peening is a commercially proven technology that has been shown to create compressive residual stress in both unstressed materials, as well as materials containing tensile surface residual stresses generated by welding. Lawrence Livermore National Laboratory (LLNL) has developed the laser peening process and the associated hardware for use by the YMP. Upon completion of the testing and engineering phases, LLNL will transfer the laser peening technology to U.S. industry and assist DOE in developing vendors to supply production units to be installed at the YMP facilities.

The overall testing effort is divided into two phases. Phase I of this project consisted of a study into the effectiveness of laser peening in generating compressive stress in small Alloy 22 base metal coupons and converting tensile stress in Alloy 22 welds into compressive residual stress. Particular emphasis was placed on optimization of process parameters to achieve compressive residual stress at greater depths than has currently been demonstrated. The process parameters studied included the laser irradiance (power per area), the laser pulse duration, the number of peening layers, the effect of the ablative layer (described below), and the effect of part thickness. Additionally, the effect of two process parameters, the number of peening layers and the effect of the ablative layer, was evaluated by measuring general corrosion resistance of peened and unpeened Alloy 22 coupons with an electrochemical polarization method. This initial effort (\$95,000) was started in August 22, 2002 and completed on September 30, 2002.

Phase II (\$70,000) of this project was started on September 14, 2002. Using the parameters determined from the initial phase (and listed in Appendix A), five welded flat plate specimens (three plates, 3/8 inch thick and two plates, 1 inch thick) were laser peened at LLNL. These peened plates, identified as Stress Mitigation Welded Specimens, were shipped to qualified YMP suppliers (Chalk River Neutron Diffraction facility, and Lambda Research Inc.) for residual stress measurements.

This report summarizes technical achievements made in Phase I. It is evident from this work that laser peening is a mature technology for YMP to effectively mitigate the potential for stress corrosion cracking in Alloy 22 welds.

Methods

Laser Peening

Laser peening was performed with LLNL's high-energy, flash lamp pumped, pulsed Nd-glass laser with SBS phase conjugation. The laser system (shown in Figure 1) is a 150 W unit with an output of 25 J/pulse at 6 Hz. This is 25 times the pulse rate of competing technologies suitable for laser peening, which leads to a corresponding decrease in processing time and expense. A laser of similar design is currently being operated (five days per week and 24 hours a day) at Metal Improvement Company's Laser Peening Facility to peen turbine blades for the aerospace industry.

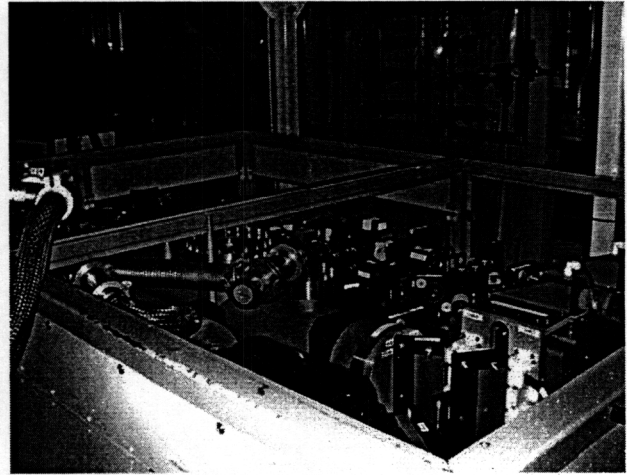
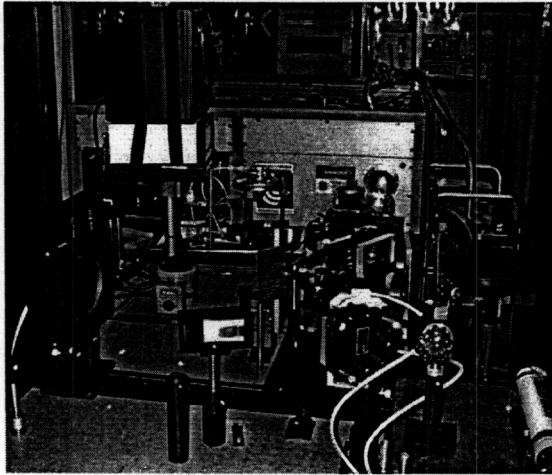


Figure 1: Laser system at Lawrence Livermore National Lab

The following table summarizes the general operating parameters of the LLNL laser peening system:

Table 1: Laser system operating characteristics

Parameter	Variable	Value
Laser pulse energy	E	up to 25 J
FWHM (full width half maximum) pulse duration	t	20 ± 6 ns
0-50% rise time	t_{r50}	3 ± 1 ns
Peening spot shape (laser cross section at target)	(none)	nominally square
Spot edge dimension	d	2 to 5 mm
Spot uniformity (energy variation over the central 80% of the spot area)	m	$\leq \pm 20\%$

Laser peening requires only a nominal cleaning and degreasing of the surface to remove residue from fabrication and transport, prior to processing. The process is shown schematically in Figure 2. The surface of the substrate is covered with an ablative layer, typically tape or paint, which serves the dual purpose of providing insulation between the laser pulse and the workpiece, and acts as the material source for plasma generation in the laser peening process. Alternatively, the surface of the workpiece can be ablated directly if desired, eliminating the need for the tape layer. On top of the absorption layer is a thin, inertial layer, typically a laminar fluid flow,

transparent to the laser light that acts as a tamper, or as a confinement “cover” for the pressure that will develop. When the laser beam illuminates the surface, it is absorbed and rapidly forms high intensity plasma. The expansion of the plasma is confined by the tamping layer and builds to a pressure of roughly a million pounds per square inch. This high pressure results in a shock wave that travels into the workpiece, straining the material. Since the laser intensity is tailored to create a shock that is above the yield strength of the metal, a permanent compressive residual stress is induced. Thus the process can very effectively convert tensile stresses in the metal to strong and relatively deep compressive stress. Fundamentally, this is the same process employed by shot peening; laser peening develops far higher pressures than shot peening however, while causing less surface damage.

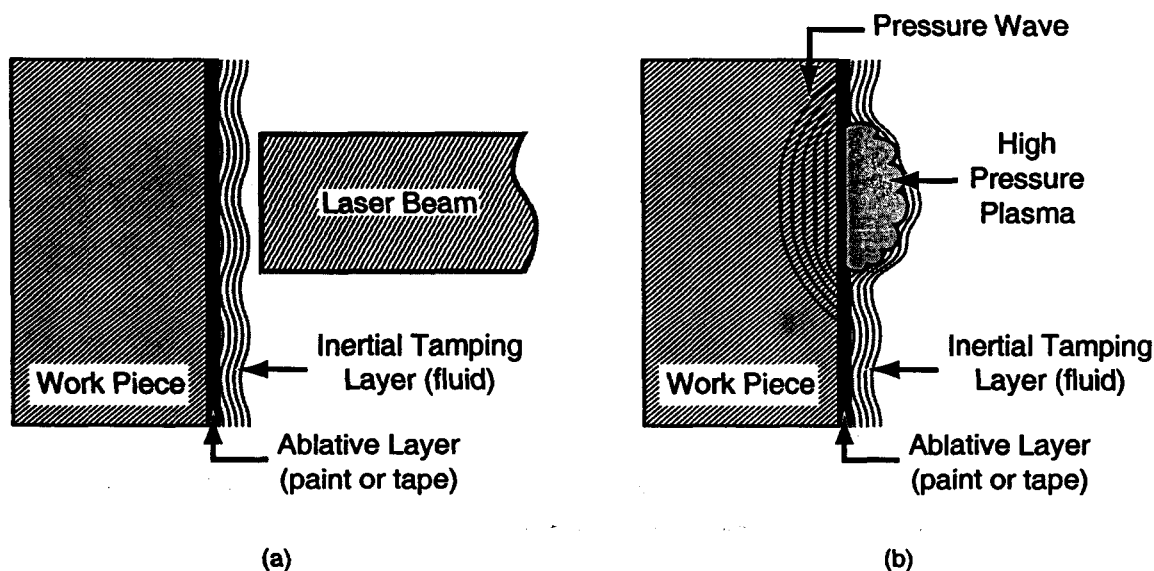


Figure 2: Schematic of the laser peening process

Measurement of Residual Stresses

There are numerous methods available for measuring residual stress in metals. Some of these methods include diffraction techniques, either using x-ray or neutron sources, or physical measurements of strain, including the slitting, contour, ring core or hole drilling methods. LLNL does not have the capability to readily make these measurements on site. TEC Materials Testing Laboratory (TEC) was contracted to perform residual stress measurements using the x-ray diffraction (XRD) technique. The XRD results showed a large amount of scatter that may be caused by the large and non-uniform grain structure of Alloy 22. Additional attempts were made to measure the stress profile (through the depth) of laser peened Alloy 22 coupons using mechanical methods. Dr. Michael R. Hill and his students (from the University of California, Davis) used the slitting and the contour methods to measure these residual stress profiles. These methods are summarized below, and discussed in more detail in Appendix B.

X-ray diffraction: Residual stress measurements were made by TEC on Bragg-Brentano geometry diffractometers, and the data are collected by step scanning using computer controlled diffractometers instrumented with scintillation or solid state Si (Li) detector systems to eliminate background fluorescence. The macroscopic residual stresses are then calculated from the strain measured in the crystal lattice by employing x-ray elastic constants determined empirically.

Residual stress measurements on Alloy 22 coupons were made at the surface and several depths beneath the surface. The various depths are exposed by electropolishing techniques. X-ray diffraction data obtained as a function of depth are then corrected for the influence of the penetration of the radiation into the subsurface stress gradient. The residual stress calculated at each depth beneath the surface of the sample is corrected for stress relaxation due to the removal of stressed material by electropolishing.

Microhardness measurements: Another possible method for estimating the depth of residual stress in treated components is through the measurement of the material hardness. Vickers microhardness scans were performed at LLNL through the depth of the part on a surface cut by wire electric discharge machining (EDM), and subsequently polished. This method does not quantify residual stress but is assumed to act as an indicator of cold work. Comparing the relative depth of cold work between coupons is then assumed to represent the relative depth of residual stress. The orientation of the hardness scan relative to the part is shown in the following figure.

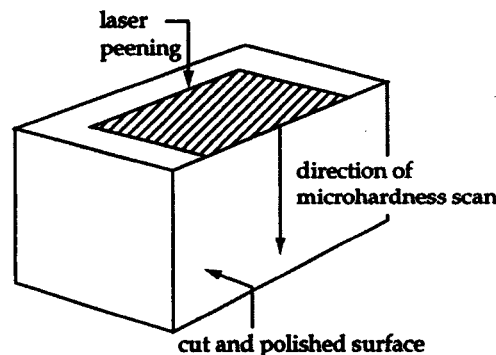


Figure 3: Schematic of microhardness measurements

Slitting method: The general procedure for slitting (also called the crack compliance method) (Prime, 1999) is to gradually extend a slit into the specimen surface and measure near-slit strain as a function of slit depth. Strain due to slitting is measured using metallic foil gages placed near the slit and the slits are cut using wire EDM. Strain versus slit depth data are then input to an inverse elastic analysis to compute the variation of pre-slit residual stress with depth from the surface (i.e., the stress profile). The method assumes elasticity and an invariant stress distribution along the axis of the slit (both valid for these measurements), and provides a one-dimensional, through thickness measurement of the residual stress present in the body, prior to the slitting experiment. Please refer to the attachment in Appendix B for a complete description of the slitting method.

Contour method: In this method, the component of interest is cut in two using wire EDM. Following cutting, the cut surfaces on each of the two halves of the part are measured (typically with a coordinate measuring machine) to determine the surface profile normal to the cut. The original residual stresses are then calculated from the measured surface contour using a straightforward finite element model. The elastic material properties of Alloy 22 were required for the calculation and these were assumed to be $E = 207 \text{ GPa}$ and $\nu = 0.3$ (as found in the Hastelloy 22 product information pamphlet). The contour method is a powerful tool for measuring residual stresses in welds, since it provides a two dimensional map of the stress component normal to the cutting plane. While it does assume elastic response, it allows for stress

variation along both directions within the cutting plane. Please refer to the attachment in Appendix B for a complete description of the contour method.

The x-ray diffraction method was primarily used to measure the residual stress on the surface of Alloy 22 samples, where the mechanical release methods have limited capability. Slitting and surface contour methods were used selectively to determine the residual stress profile (in depth) beneath the surface of base metal and welded samples.

Alloy 22 Weldment Coupons

The effects of laser peening were evaluated in actual Alloy 22 weldments using samples fabricated from a butt-welded 33 mm (1.3 inch) thick Alloy 22 plate, D-22 (HT 059902CL1, welded by Framatome Technologies Inc.). The initial plate was approximately 813 mm (32 inch) long (longitudinal) and 201 mm (7.9 inch) across (transverse). This plate was cut into four 190 mm (7.5 inch) long, full-width samples, and two of these were used in this work

Laser peening was applied to one surface of one sample. The peened region was centered on the weld and was 76 mm (3 inch) long and 100 mm (4 inch) wide. A picture of half of each sample is shown in Figure 4, after cutting in half, as required by the contour method. The cutting of the specimens was performed on a Sodick AQ325L linear motor driven wire EDM by a commercial vendor, and measurement of the cut surfaces was performed on a high-precision Leitz PMM 12106 coordinate measuring machine (CMM) at LLNL. A complete description of the contour method is given in Appendix B.

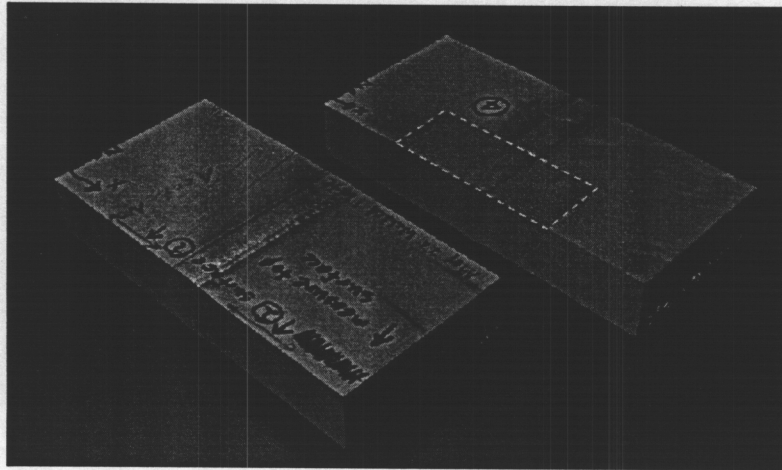


Figure 4: Unpeened (left) and laser peened (right) samples following sectioning required by the contour method (the peened region is rectangular and is indicated by a dashed line).

Alloy 22 Base Metal Coupons

A parametric study of laser peening residual stresses as a function of several process parameters was performed in Alloy 22 base metal specimens. The baseline method for measurement of residual stresses in this study was the slitting method; comparison measurements of through thickness residual stress profile, along with measurements of surface residual stress for a number of laser peening conditions were made with x-ray diffraction. Additionally, microhardness measurements were made on three coupons previously measured with slitting, to determine the value of the microhardness technique.

There are numerous parameters that play a role in determining the residual stress state in a laser peened material. In this study, the following parameters were investigated:

- Laser irradiance (power per area)
 - 13.5 mm thick coupons were treated with irradiances of 7 and 10 GW/cm²;
- Number of peening layers
 - 9.5 mm thick coupons were treated with 2, 5, and 10 layers of peening
 - 20.8 mm thick coupons were treated with 10 and 20 layers of peening;
- Effect of a backing plate, which is typically used to support relatively thin coupons during laser peening
 - 9.5 mm thick coupons were treated with and without a backing plate
- Effect of the ablative layer:
 - Peening was applied to a 13.5 mm thick coupon with the standard aluminum tape ablative layer applied between each layer of peening
 - Peening was applied to a 13.5 mm thick coupon without aluminum tape (coupon surface is ablated directly) for 10 layers, followed by two additional layers with normal aluminum tape ablative layer
 - Peening was applied to a 13.5 mm thick coupon without aluminum tape for 12 layers

Corrosion Testing

Electrochemical polarization tests were carried out in a Simulated Acidified Water (SAW) solution at a nominal temperature of 90°C and pH of 2.7. Tests were performed on Alloy 22 base metal specimens with 2, 4, and 10 layers of laser peening, along with corresponding control coupons polished at the same time, but with no laser peening. De-aeration with pre-purified N₂ was performed 1-hour prior to testing as well as throughout the test at a flow rate of 100 cc/min. Scan rates were maintained to the ASTM standard value of 0.1667 mV/s.

Results

Alloy 22 Weldment Coupons

The following contour plot of the longitudinal component of residual stress in the unpeened sample shows typical trends for a double-sided butt weld (Figure 5a). Tensile stresses at the weld center are largest just below the weld surface and are smallest at the mid-thickness. Residual stresses on the top and bottom weld surfaces are tensile at the weld center and gradually become compressive outside the weld bead. The maximum tensile stress is similar to reported values of the tensile yield strength of Alloy 22 plate.

A contour plot of residual stress in the laser peened sample shows a region of large and uniform compressive stress within the peened area (Figure 5b). Outside the peened area, residual stresses are similar to those in the unpeened sample.

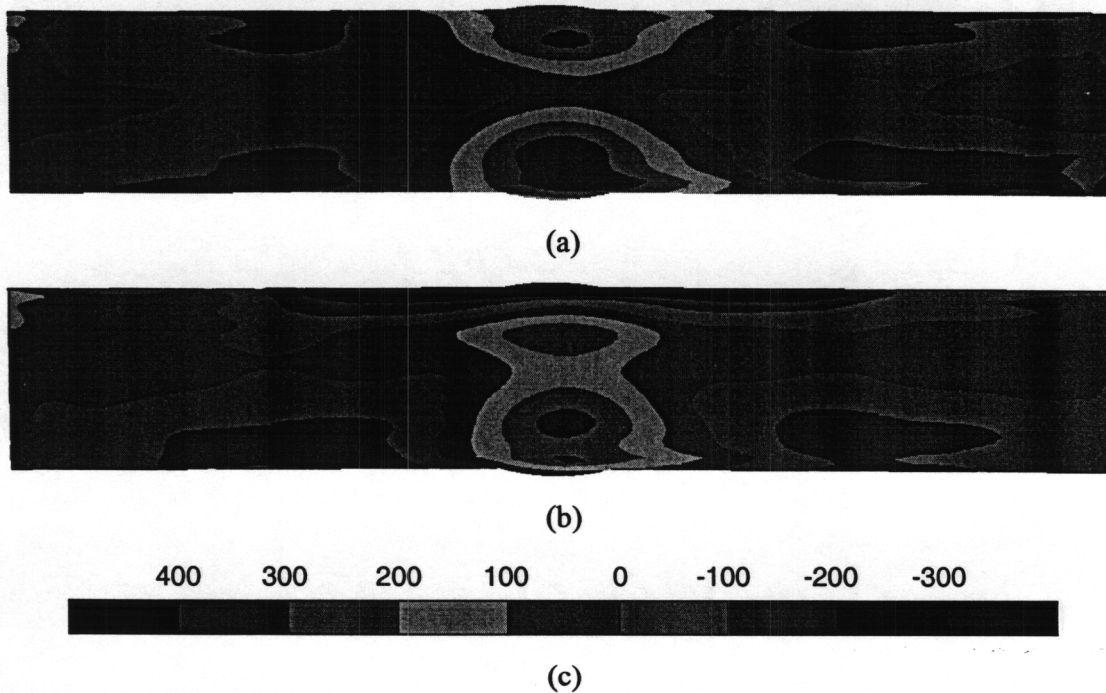


Figure 5: (a) Longitudinal component of residual stress present in the weld before laser peening, (b) Longitudinal component of residual stress present in the weld after laser peening surface treatment (laser peened surface is on the top of the figure), (c) Color map for residual stress magnitude (MPa)

Line plots of longitudinal residual stress versus depth from the surface more precisely illustrate residual stress in the unpeened weld and the effect of peening (Figure 6 through Figure 8). Line plots were prepared at three locations in the weld: at the center of the weld bead (Figure 6), at the right weld toe (Figure 7), and outside of the welded region (30 mm (1.2 inch) from the weld center, Figure 8). These plots clearly show the effect of laser peening, and indicate that it produces deep compressive stress in both weld and base metals and at the geometrically discontinuous weld toe.

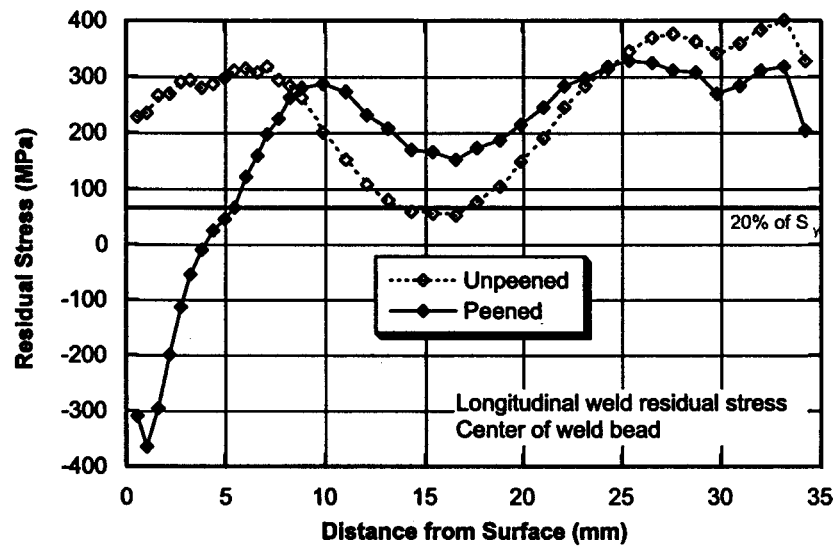


Figure 6: Longitudinal component of residual stress at the center of the weld bead with and without laser peening

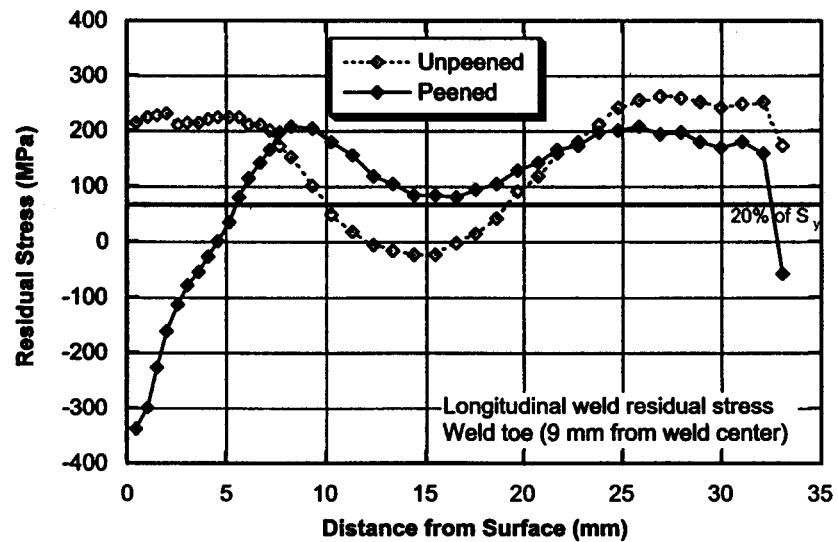


Figure 7: Longitudinal component of residual stress at the right weld toe, with and without laser peening

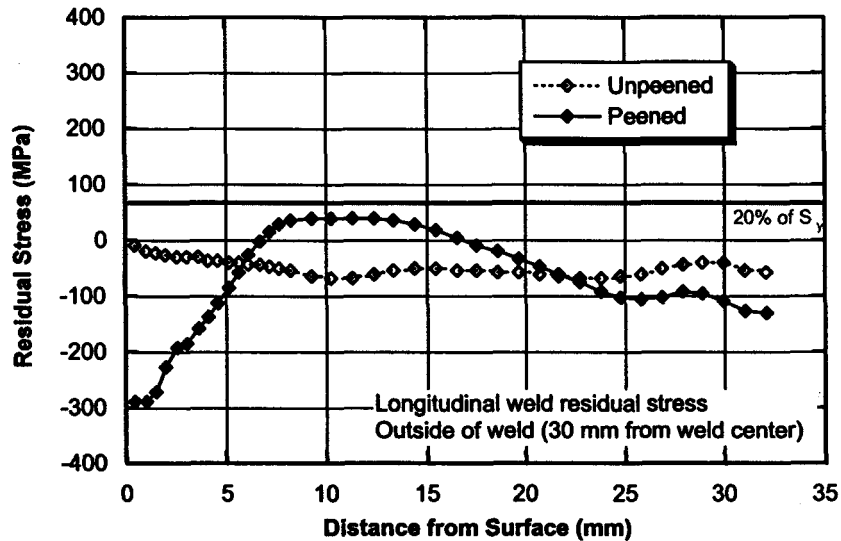


Figure 8: Longitudinal component of residual stress outside the weld region (30 mm from the weld center) with and without laser peening

Corrosion Testing

Electrochemical polarization results thus far have shown an increase in corrosion resistance for laser-peened Alloy 22 base metal samples relative to their untreated counterparts. This increase in corrosion resistance can be assessed according to a lower average corrosion rate obtained using the polarization resistance method. Figure 9 is a comparison of average corrosion rates of various Alloy 22 sample types exposed to a Simulated Acidified Water (SAW) medium at 90°C. In each case 1 hour of open circuit monitoring occurred before polarization resistance experiments were carried out. The number to the far right in parentheses refers to the quantity of trials performed on each sample type. The values shown in Figure 9 should not be perceived as absolute corrosion rates but rather relative values to provide a means of comparison.

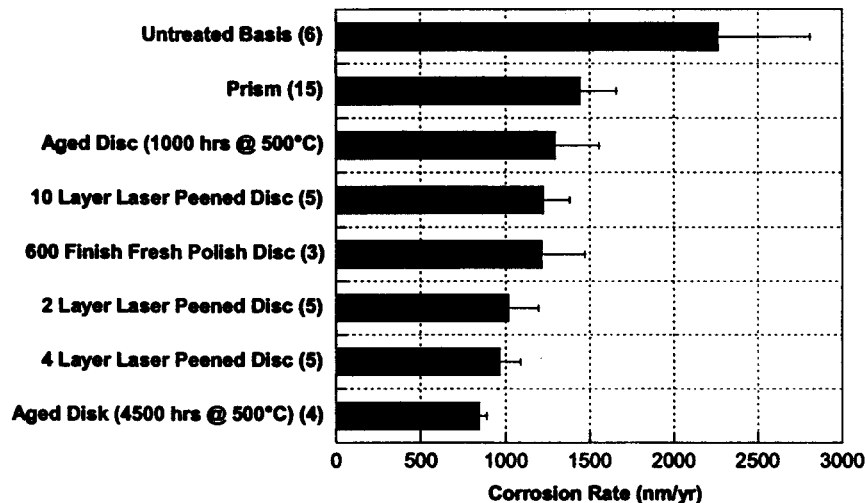


Figure 9 Average Corrosion Rates obtained for Alloy 22 in 90°C SAW

According to Figure 9 average corrosion rate values are approximately the same for the 2 layer, 4 layer, and 10 layer laser peened surfaces. But in general, average corrosion rates for the untreated basis used in this study show higher corrosion rates.

The potentiodynamic polarization curves shown in Figure 10 exhibit lower passive current densities for the laser-peened samples compared to the as polished basis. But there is no apparent decrease in passive current density between the sample that received 4 layers versus 2 layers of laser peening. However, a slightly lower passive current density can be seen for the 10 layers treated sample when examining the active-passive region.

Contrary to similar studies performed on stainless steel alloys, the polarization curves in Figure 10 are devoid of any critical pitting potential. Instead, a transpassive breakdown (E_{crit}) of the metal is the result of imposing a more anodic potential on Alloy 22. For each curve shown in Figure 10 transpassivity occurs at roughly the same potential slightly beyond 600 mV_{SSC}.

For future studies it would be valuable to compare untreated weld samples versus treated weld samples. In addition, choosing a more aggressive environment such as 9M CaCl₂ solution at 150°C may exhibit significant differences in corrosion behavior according to key electrochemical parameters such as E_{corr} and E_{crit} .

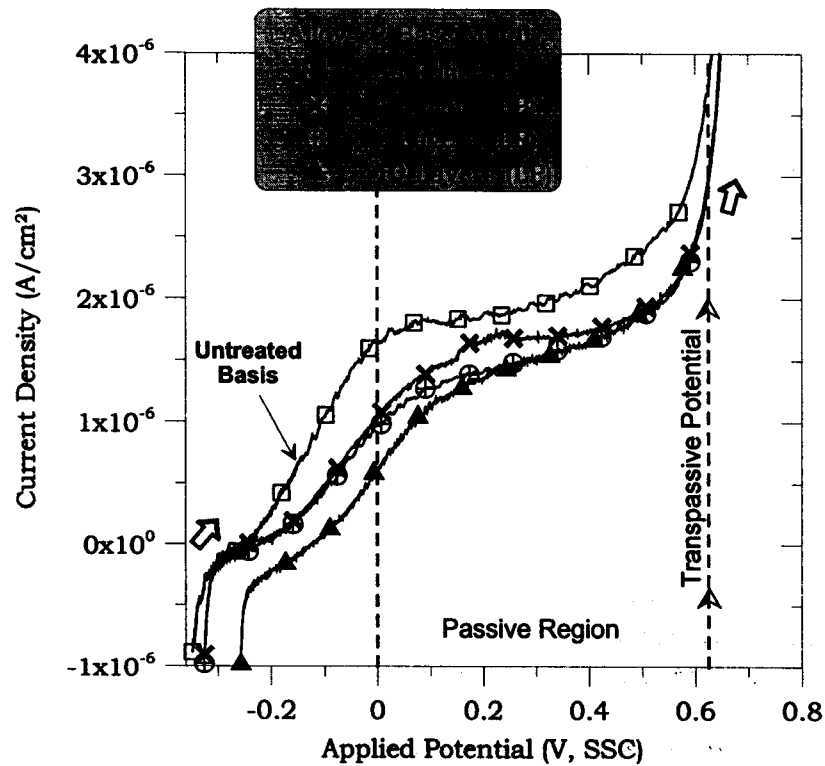


Figure 10: Potentiodynamic Polarization of Alloy 22 in 90°C SAW

Alloy 22 Base Metal Coupons

High magnitude compressive surface residual stress is easily attained in Alloy 22 with a wide variety of laser parameters. The results of the x-ray surface residual stress measurements are summarized in the following table. The only cases where the measured stress is not near or above yield (nominally 372 MPa at room temperature in an unworked state) are the cases where the coupon was peened without the ablative layer of tape (explained further below). Note that the magnitude of the surface stress is not the most important criteria for this application; it is more desirable that the residual stress extends deep into the part.

Table 2: Surface residual stress measurements by x-ray diffraction

Treatment	First X-ray Surface Residual Stress Measurement (MPa)	Second X-ray Surface Residual Stress Measurement (MPa)
15 ns, 12 GW/cm ² , 1 layer	-360±26	N/A
15 ns, 12 GW/cm ² , 2 layers	-430±30	N/A
15 ns, 12 GW/cm ² , 3 layers	-430±30	N/A
15 ns, 12 GW/cm ² , 4 layers	-430±30	N/A
25 ns, 10 GW/cm ² , 10 layers	-372±20	N/A
25 ns, 10 GW/cm ² , 10 layers without tape, followed by 2 layers with tape	-377±21.5	-179±18.3
25 ns, 10 GW/cm ² , 12 layers without tape	-23±15.9	-107±16.1

The residual stress profiles presented in Figure 11 through Figure 15 were measured using the slitting method. Figure 11 shows the effect of laser irradiance on the residual stress state generated by laser peening. The surface residual stresses are comparable for both values of laser irradiance investigated, but treatment with 10 GW/cm² drives residual stress about to about 3 mm, or about 50% deeper than 7 GW/cm². More data are currently being collected for coupons peened with 7, 10, and 13 GW/cm², with consistent laser spot size and pulse lengths to obtain a more complete data set.

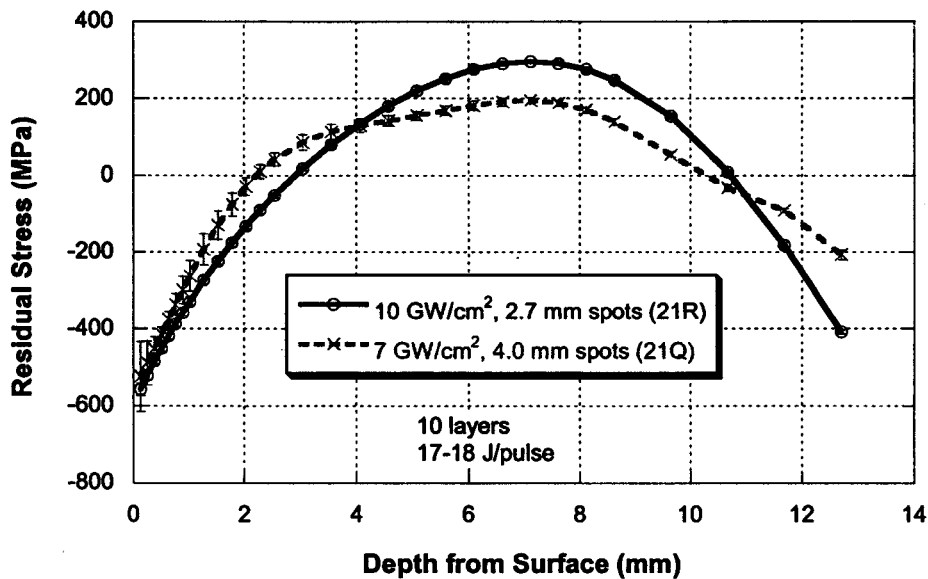


Figure 11: Residual stress versus depth as both spot size, and irradiance (power per area) are varied in 13.5 mm coupons

The interaction between the number of peening layers and the residual stress profile is under continuing investigation. Additional measurements of residual stress with 2 and 5 layers of

peening will be made in 20.8 mm thick coupons to evaluate and compare the effect of the number of peening layers in a single specimen geometry. The current results indicate that in thin coupons (approximately 9 mm thick) residual stresses do not increase significantly in magnitude by increasing the number of peening layers (Figure 12). Likewise, the increase in residual stress magnitude in 20.8 mm coupons (Figure 13) is small when the number of peening layers is increased from 10 to 20.

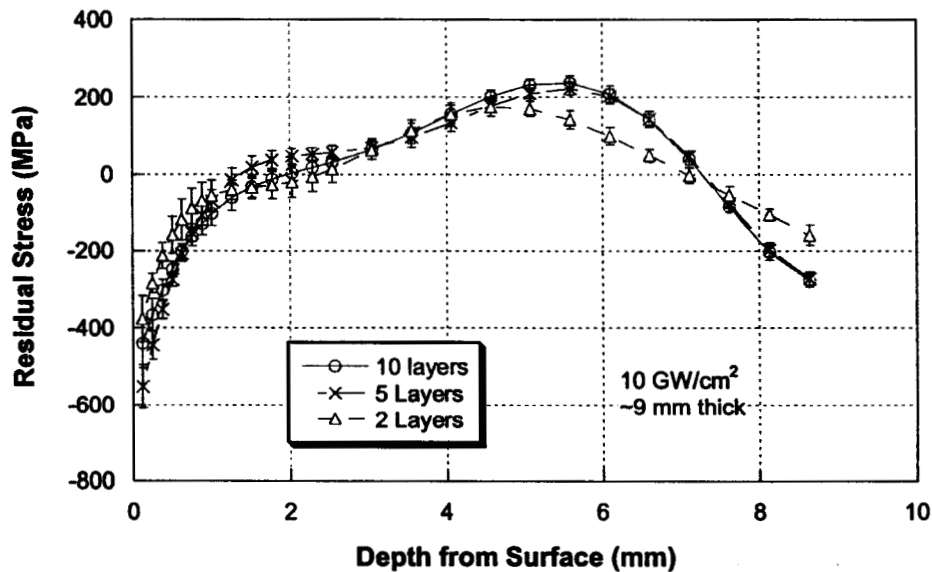


Figure 12: Residual stress versus depth as a function of number of peening layers in 9 mm coupons

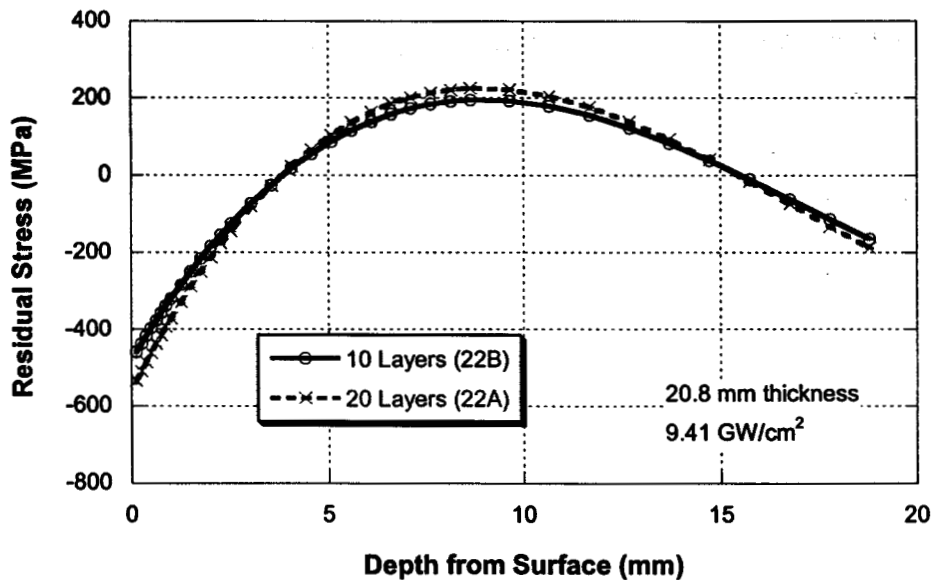


Figure 13: Residual stress versus depth as a function of number of peening layers in 20.8 mm coupons

The stress profile when the ablative tape layer is used only on the last two layers is not significantly different from the normal peening, where tape is used on every layer (Figure 14). Peening without taping between each layer would represent a significant savings in processing time, therefore cost. Peening without taping at any time results in a lower magnitude stress near the surface, although still compressive. The through depth residual stress measurements by the slitting method were augmented by surface stress measurements by x-ray diffraction method, the results of which are listed in Table 2. While the values of residual stress are lower in magnitude for coupons processed without an ablative coating between each layer of peening, they do remain compressive. When tape is used on the last two layers, the surface stress is approximately the same as for normal peening.

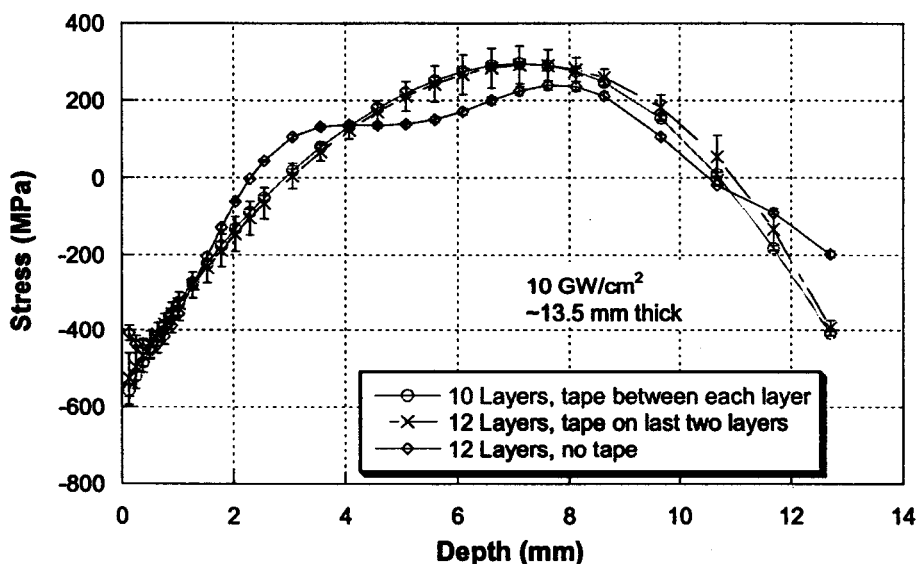


Figure 14: Residual stress as a function of depth with different protocols in applying the ablative layer

The presence of a backing plate does appear to play a significant role in the final residual stress state in thin coupons. While the surface stress is higher in magnitude without a backing plate, compressive stress reaches a slightly greater depth when a backing plate is used (Figure 15). While research is continuing to quantify this effect, this result agrees with the findings regarding depth of residual stress as a function of coupon thickness, which is discussed below.

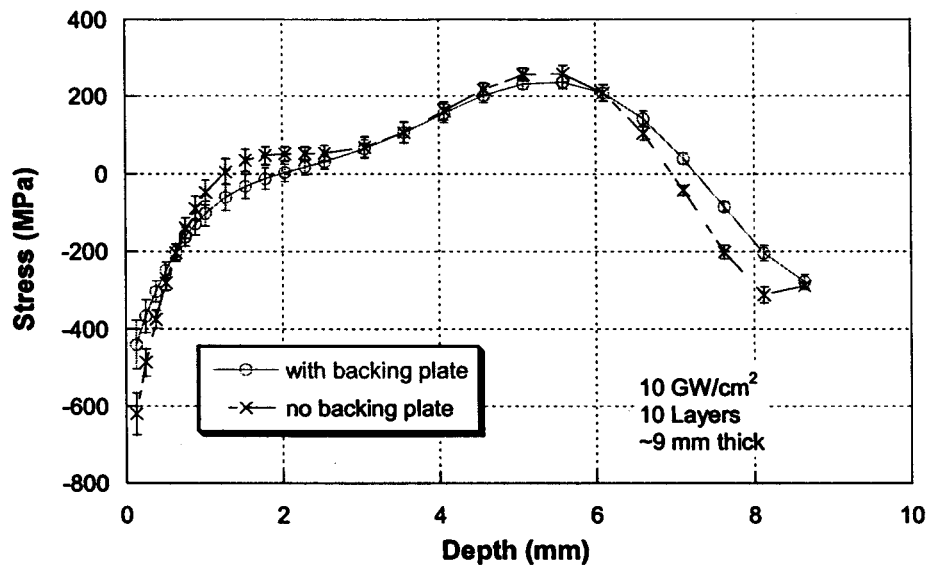


Figure 15: Residual stress as a function of depth for parts processed with and without the support of a backing block

Comparison of Residual Stress Measurement Methods

Measurements of residual stress as a function of depth performed using x-ray diffraction and layer removal provided data from which no conclusions could be drawn (Figure 16). There is no identifiable relationship between the number of peening layers and the resultant residual stress, nor do the results provided by x-ray diffraction seem physically plausible.

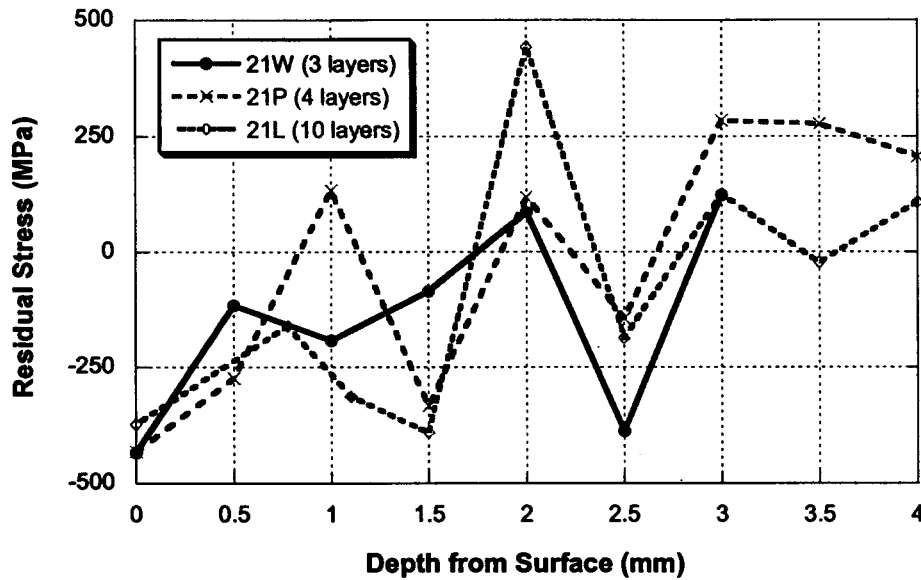


Figure 16: Residual stress as a function of depth for different numbers of peening layers, measured with x-ray diffraction

A direct comparison of the residual stress data measured by x-ray diffraction and slitting methods suggests that there is less inherent error in this application when using the slitting method (Figure 17). Measurements were made on two identically prepared coupons with the two methods. It is evident that the data from the slitting method pass through the trend of the x-ray data, and provide a more reasonable stress result. Additionally, slitting provides a residual stress record through nearly the entire thickness of the part, which would be costly and time consuming to attempt with x-ray diffraction.

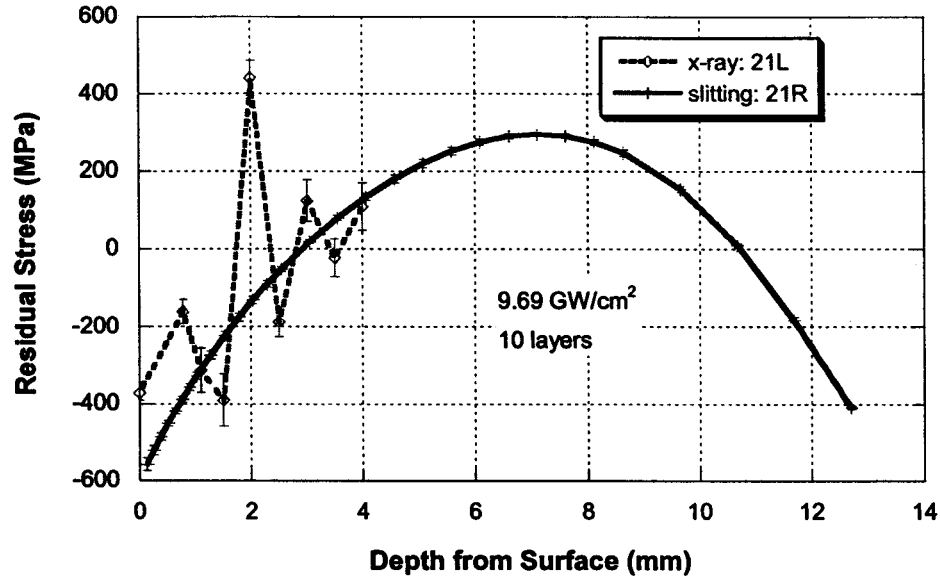


Figure 17: Residual stress with depth as measured by the slitting method and x-ray diffraction

Microhardness scans were performed through the depth on the cut and polished surfaces of three laser peened coupons (Figure 18). There is a significant hardness elevation through the first 2.5 mm in all three coupon thicknesses. The hardness continues to drop through approximately 9 mm in the thinner, 14 mm coupon; in the 20 mm coupons, the hardness appears to drop through the entire measurement depth. The unsmooth variations present in the data, along with the fact that the technique does not provide a measurement of residual stress, reduce the efficacy of this method for inspecting processed Alloy 22 coupons. For reference, results from the slitting method indicate that compressive residual stress extended to approximately 4 mm in the 20 mm thick coupons, and to approximately 3 mm in the 14 mm coupon.

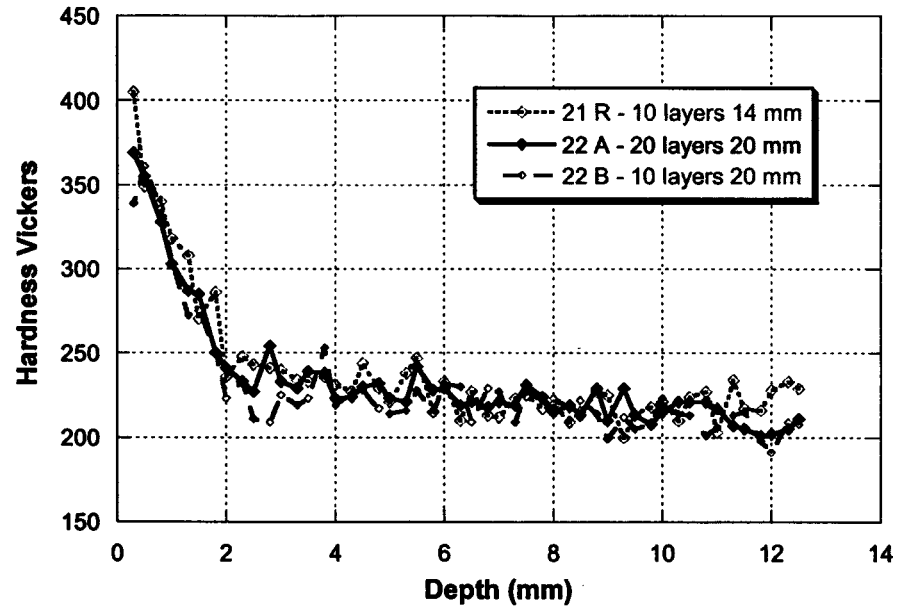


Figure 18: Microhardness traverses in three laser peened coupons

Discussion

Alloy 22 Weldment Coupons

The depths of compressive stress in the laser peened samples were quantified from the line plots of residual stress versus depth measured with the contour method. Depth of compressive stress was determined in two ways, from both the depth at zero residual stress and the depth at a tensile stress equal to 20% yield strength. The yield strength of the welded material was assumed to be 372 MPa (54 ksi), which is the room temperature yield strength in un-welded plate, as reported by a material vendor (found in the Hastelloy 22 product information pamphlet). The depths of compressive residual stress in the peened weld, from each of the depth definitions and at each position where a line plot was prepared, are given in Table 3.

Table 3: Summary information on depth of compressive stress

Location	Zero crossing (mm)	20% yield crossing (mm)
Weld bead center	4.0	5.6
Weld bead toe	4.6	5.7
Outside of weld region	6.8	Does not exceed

The line plots also illustrate an expected trend that indicates consistency between the two residual stress measurements. Since the two welded samples were removed from the same long weld, and the weld was likely prepared by welding continuously along the length, the two samples should have contained the same residual stresses before peening. Further, the earlier small coupon residual stress measurements suggest that the laser peening process employed does not plastically deform material more than 15 mm from the peened surface. Therefore, stresses more than 15 mm from the peened surface should be similar in the unpeened and peened welds. Considering the equilibrium conditions of elasticity theory, peening residual stress is equilibrated by uniform tension and bending across the thickness of the welded plate. It should therefore be expected that residual stresses in the unpeened and peened welds, at distances more than 15 mm from the peened surface, should differ by only a linear function with depth. This trend is evident in Figure 6 through Figure 8, and is quite clear when the difference in residual stress between peened and unpeened samples is plotted.

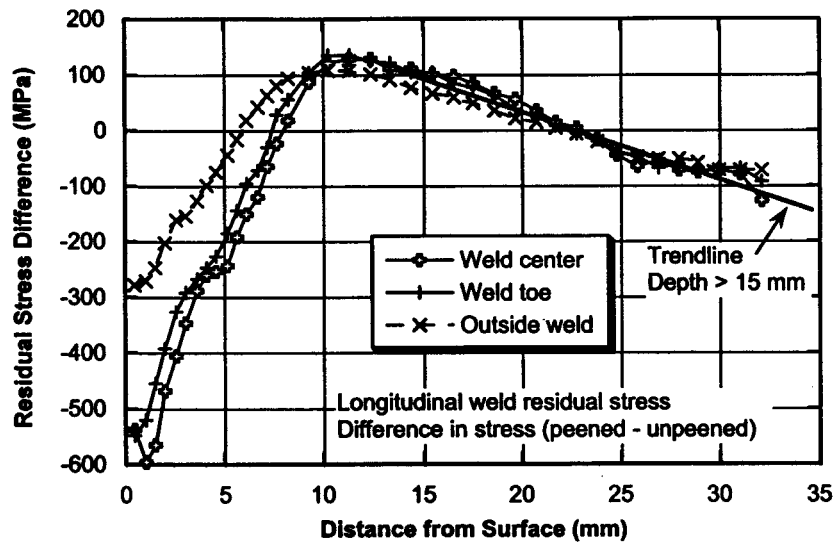


Figure 19: Difference between the longitudinal component of residual stress in laser peened and unpeened weld samples, at various positions transverse to the weld

The stress differences (as shown in Figure 19) also indicate that laser peening has a larger effect in regions of initially tensile weld residual stress. This may be due to the effect of initial weld residual stress on plastic deformation induced by laser peening, or by a limit to the maximum level of compressive stress that can be introduced by laser peening. The latter possibility is supported by the fact that the maximum compressive residual stresses in Figure 6 through Figure 8 are nearly equal.

Corrosion Testing

Decreasing the general corrosion rate of Alloy 22 is a very favorable effect of the laser peening process. Models of the corrosion of YMP waste packages suggest that up to 5 mm of the waste package surface could be removed by general corrosion over the design life of 10,000 years (Farmer, 2000). To mitigate the potential for SCC, the compressive residual stress generated by laser peening must be deep enough to ensure that the new, exposed surface remains in a state of compressive stress, even after thousands of years of general corrosion. If the general corrosion rate is slowed dramatically, 5 mm of compressive residual stress will mitigate the potential for SCC for a significantly longer time.

Alloy 22 Base Metal Coupons

The results of the slitting method measurements in specimens of various thickness show that the depth of compressive residual stress is directly affected by the thickness of the coupon undergoing laser peening. Since the stresses in an unloaded part must exist in equilibrium, tensile stress must occur inside the part, to balance the compressive stress induced by laser peening. Laser peening can attain deeper residual stresses in a thick section than in a relatively thinner one. This is demonstrated in the figure below, which plots the depth of compressive residual stress, quantified as the point where the measured stress profile passes through zero stress, versus

four different specimen thicknesses investigated (note that for the fourth point, the depth of residual stress is reduced to 6 mm from 6.8 listed in Table 3; the material was in a state of compressive stress prior to peening because of the welding process. At a depth of 6 mm, the residual stress after peening is equal to the level present prior to peening). All the specimens shown were peened with the same laser parameters. The trend is close to linear through all the specimen sizes, indicating that the attainable depth of residual stress is driven by part geometry, as well as the surface treatment.

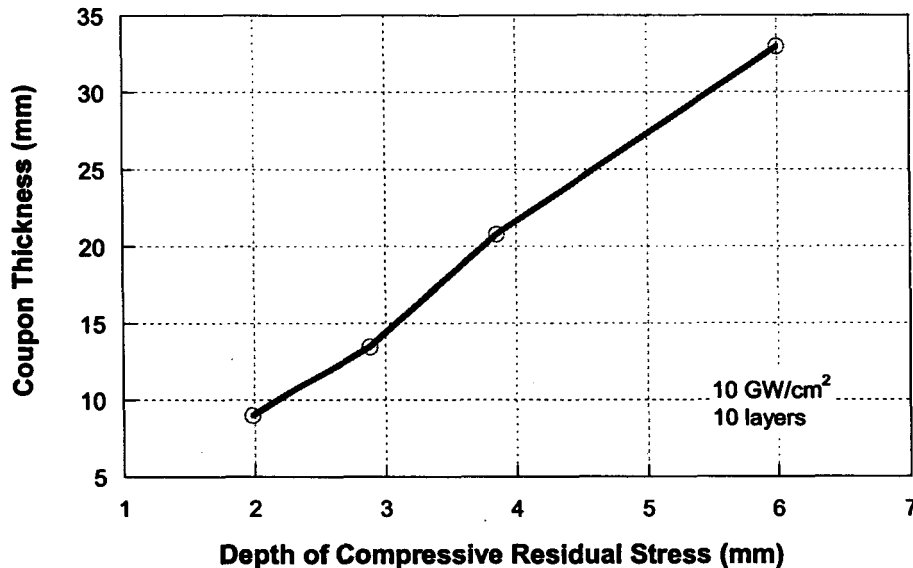


Figure 20: Depth of compressive residual stress as a function of coupon thickness

Understanding this result is critical; the attainable depth of residual stress relies heavily on the thickness and geometry of the part undergoing laser peening. It is very challenging to drive compressive residual stress through more than a quarter of a simple plate thickness, since a substantial portion of the cross section is required to react the effects of the compressive residual stress introduced by laser peening. In a geometry like the stress mitigation welded coupons, where a relatively thin plate is supported by sizable welded backing structure, deeper compressive residual stresses could be achieved in a similar plate thickness; the backing structure will increase the effective cross sectional area, thereby increasing the depth of compressive residual stress that can be supported. Note that in the current waste package design, the outer lid will be 25 mm thick (Plinski, 2001). From Figure 20, the current laser peening settings should be able to generate compressive residual stress to a depth of nearly 5 mm, or greater because the outer lid is supported by substantial material.

Comparison of Residual Stress Measurement Methods

Of the four methods used to quantify the depth extent of residual stress in both Alloy 22 weldments and base metal coupons, the mechanical release methods, the slitting and contour methods, provide the most satisfactory results. These methods use equipment commonly available in precision machine shops and yield powerful data with relatively little expense. Release methods are particularly effective in this application, since diffraction methods are difficult to implement in welds due to microstructural variations between the weld and parent

material. X-ray diffraction does provide data for surface residual stresses that can't be measured with the release methods; however, the principal figure of merit for a residual stress state for this application is depth of residual stress, rather than surface level. As shown in Figure 17, x-ray did not provide reasonable results for this measurement. The fourth method used in this work, the microhardness technique, makes the broad assumption that hardness can be related directly to the residual stress state, which is not the case. Approximations of the total depth of plasticity from the microhardness data (the depth where the microhardness plateaus) do correlate with estimates of depth of plasticity based on the residual stress profile, as discussed above in reference to Alloy 22 weldments.

Concepts for Deployment of Laser Peening at Yucca Mountain

The Laser Peening System can commence operation after conclusion of the GTAW (Gas Tungsten Arc Welding) of the closure lid to the Disposal Container (DC). This would include completion of the weld surface examination/volumetric inspection (SE/VI) (Knapp, 2001). All Laser Peening operations would be conducted at the Surface Facilities and are an integral part of the Closure Cell Control System.

The Laser Peening System is divided into three main parts: the laser system, the laser transport system and the laser beam control/scanning system. The following will describe each of the three subsystems that comprise the Laser Peening System.

The laser system is a system of optics, amplifiers, electronics and ancillary equipment all designed and integrated to produce a high quality, high reliability laser beam. Figure 1 provides photos of such a system currently working at Lawrence Livermore National Laboratory (LLNL). A typical laser system would be enclosed in a Class 1000 clean room, temperature controlled to ± 2 degrees C, and includes additional subsystems such as a chilled water circulation system, a pulse forming network system, power supplies and a dedicated control system.

The laser system utilizes many standard "off the shelf" components to maximize system reliability, providing a cost efficient package without sacrificing system performance. The majority of the laser system components reside on an optical table, exhibiting a footprint on the order of several office desks placed side by side. The entire laser system is stationary and can be easily accessed for any routine maintenance that may be required since it is not located in the hot cell area. Lawrence Livermore National Laboratory has deployed several of these laser systems which have demonstrated their robust design and high reliability. An example of such a laser system is one presently in use by the Metal Improvement Corporation (MIC). LLNL and MIC have established a Cooperative Research and Development Agreement (CRADA) with one another that utilizes the laser peening process to significantly extend the lifetime of turbine blades used on large passenger aircraft.

The evolution of laser systems at LLNL allows for increased performance, reductions in both footprint and correspondingly cost without any negative impact to system reliability or maintainability. An example of such a system is shown in Figure 21. Sponsored by the Space Missile Defense Command (SMDC) in Huntsville, Alabama, the purpose of this laser system is to provide in a very compact and high reliability package, sufficient power on target to destroy an incoming missile on the battlefield. This laser system utilizes "diode pumping" to develop the required amount of power in a very small footprint.

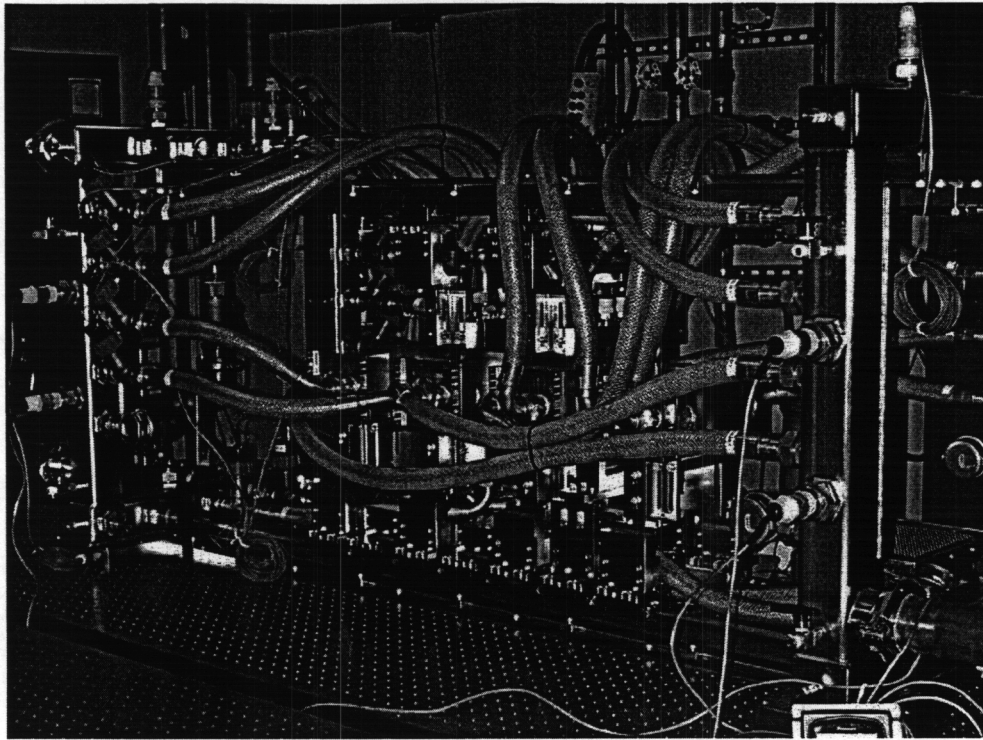


Figure 21: *The Solid State Heat Capacity Laser System (SSHCL)*

An extension of this technology could easily be developed for the Laser Peening System. Current operational laser peening pulse rates of 1 to 2 Hz could be increased an order of magnitude if not more to reduce laser peening time. In addition, laser power (utilizing diode pumped technology) could be enhanced to promote present system energy densities utilizing a larger spot size. This would again contribute to a reduction in laser peening time without any detrimental effect in performance.

Laser System Configuration Options:

- Flashlamped Pumped Laser System – present baseline configuration.
- Diode Pumped Laser System – significantly enhance performance, smaller footprint, increase laser pulse repetition rate.
- Multiple Lasers working simultaneously – decrease laser peening time, increase reliability.

The laser transport system takes the laser beam from the laser system and optically transports the laser beam into the hot cell area through a hermetically sealed optical window. This is done via a series of optical elements. Figure 22 shows conceptually the laser transport system; transporting the laser beam from its clean room into the hot cell area where the DC is located. Turning mirrors are shown to depict the type of pathway the laser beam would require, accounting for both transverse and elevation changes.

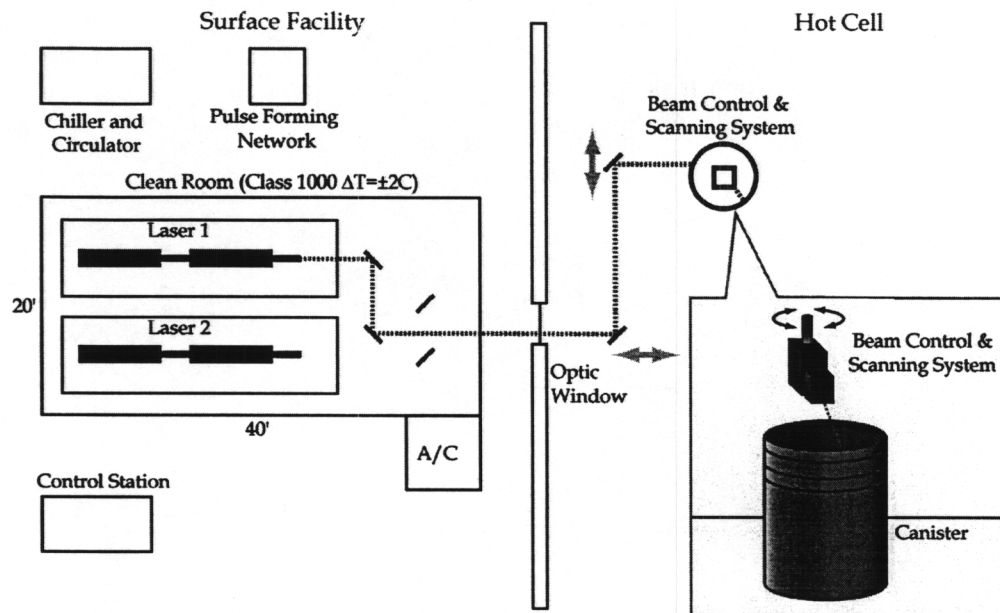


Figure 22: Laser Beam Transport System – Basic Schematic

Laser Transport System Configuration Options:

- Series of optical elements— present baseline configuration.
- Multiple laser beam paths - decrease laser peening time, increase reliability.

The Laser Beam Control/Scanning System is the 3rd major part of the total Laser Peening System. This portion of the system can be configured in several ways. The system would be incorporated into the laser peening end effector and properly aligned and indexed as it is attached to the Closure Gantry Manipulator (CGM). In this option the Disposal Container (DC) maintains a vertical axis of orientation, identical to the orientation used in the GTAW closure weld process (Knapp, 2001). Figure 23 depicts this concept as the laser beam, being directed via the laser transport system, rotates about the centerline of the DC during the laser peening process. The laser beam system rotates about a stationary DC.

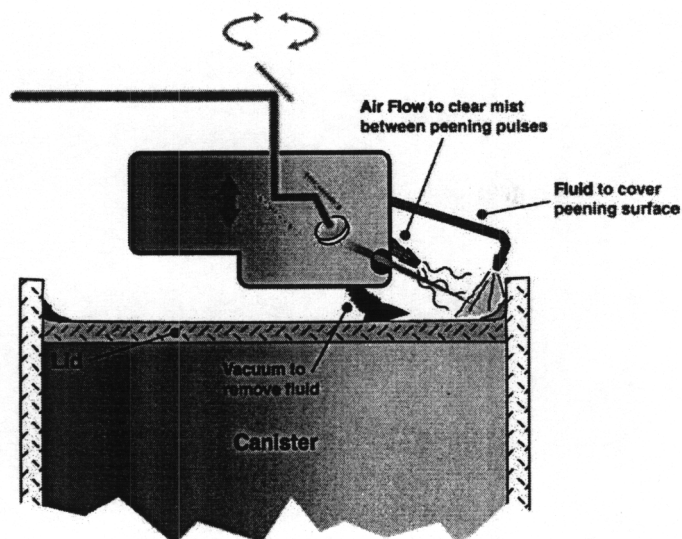


Figure 23: Vertical Orientation Laser Beam Control/Scanning System

Another configuration could have the laser peening beam held stationary in its end effector while the DC is rotated about its vertical axis. This would be accomplished by the DC resting on a small turntable that rotates about its vertical axis. Although this type of concept was eliminated from consideration for the GTAW process due to the small total run out tolerance required, the laser peening system is appreciably less sensitive to turntable run out and consequently could utilize such a system. At the present time, there is approximately 20% overlap of laser peened areas to ensure that all areas are fully and completely peened. This overlap allows for the type of small turntable run out that might be experienced in a turntable driven system. Benefits for this type of would include a mechanically simpler and consequently more reliable laser peening system without sacrificing the laser beam on-target requirement.

Another Laser Beam Control/Scanning System concept again utilizes a stationary laser beam as the DC is rotated about its horizontal axis. Figure 24 provides a conceptual understanding of this type of system. The DC is rotated so that the laser beam peens the weld circumferentially as it is rotated about its horizontal axis. Gravity is used as an aid to help direct the tamping fluid required during the laser peening operation into a suitable collection container as it circulates through the closed loop system.

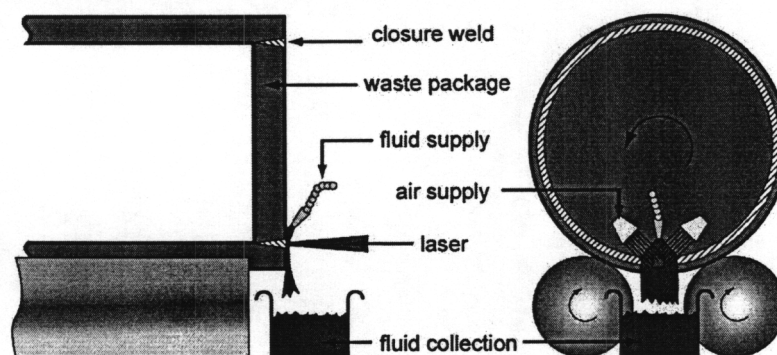


Figure 24: Horizontal Orientation Laser Beam Control/Scanning System

This concept, which once again deploys a stationary laser beam, has an additional advantage of being able to use multiple laser beams simultaneously. Envision as an example, 4 identical laser beams located around the circumference of the closure weld at the 4 positions of a clock; the 3, 6, 9 and 12 o'clock positions. All 4 laser beams would be operating in unison and would peen its corresponding quadrant worth of weld, equating to a total laser peening time of 25% of the original. This would greatly decrease the time the DC was in the hot cell area and consequently, the overall cost to provide a complete and verified closure weld. The multiple laser beam concept could also be applied to a DC mounted in a vertical axis orientation as shown in Figure 23, but the logistics of bringing in multiple laser beams from above the DC utilizing the present end effector concept seems somewhat more complicated than the horizontal axis option, but a configuration that nevertheless could be developed.

Laser Beam Control/Scanning System Configuration Options:

- Vertical Orientation Utilizing CGM End Effector – present configuration.
- Vertical Orientation with rotating DC – increase laser system reliability.
- Horizontal Orientation Utilizing a Stationary Laser Beam – increase system reliability.
- Multiple Lasers working simultaneously – decrease laser peening time, increase reliability.

After the laser peening process has been concluded, the laser peened weld joint and parent material need to be examined to ensure that the process has been done properly. Several non-destructive test methods could be employed to verify the integrity of the peened areas. High energy X-Ray radiography and phased ultrasound measurement are two potential test methods. In addition, a correlation between the depth of the compressive stress vs. the percent cold work of the material could be used to determine the final residual stress profile of the peened areas. Test strips/specimens could also be used to verify the performance of the laser peening operation. Using the surface contour method of measuring residual stress in these test coupons would provide additional support that the proper level and depth of compressive stress have been achieved.

The following is a summary table describing several examples of potential activities in support of the Laser Peening System process. All of these areas are divided into two phases; the design/proof of concept phase and the fabrication of real hardware phase to validate the proposed concept. The design phase (as shown in the table) would include the design/integration of the Laser Peening System into the overall Closure Weld Surface Facilities. The second phase of the work scope (yet to be estimated) would incorporate the process hardware into the test facilities at Idaho National Engineering and Environmental Laboratory (INEEL) so that the entire system would be fully tested and checked out before deployment.

<u><i>Activity Description</i></u>	<u><i>Benefit</i></u>	<u><i>Duration</i></u>	<u><i>Effort</i></u>
Diode Pumped Laser	Perf/Reliability	18-24 months	2 man-yrs
Multiple Laser Beams	Perf/Reliability	12-18 months	1 man-yr
Vertical DC Orientation	Perf/Reliability	12-18 months	1 man-yr
Horizontal DC Orientation	Perf/Reliability	12-18 months	1 man-yr
Laser Beam Control System Integration	Reliability & Maintainability	18-24 months	4 man-yrs
Total:			9 man-yrs

Summary

The most important findings of this work are as follows

- Laser peening produces compressive residual stress to depths on the order of 5 mm in actual Alloy 22 weldments
- The primary residual stress measurement methods used in this study, the slitting method and the contour method, produce consistent, powerful results efficiently and cost effectively. Both of these methods can be qualified, and the process has been started for the contour method.
- Preliminary results indicate that laser peening increases the general corrosion resistance of Alloy 22.
- There are a variety of options available for remote deployment of laser peening in a radioactive environment

References

Farmer, J, et al, 2000, "Modeling and Mitigation of Stress Corrosion Cracking in Closure Welds of High-Level Waste Container for Yucca Mountain", ASME.

Knapp, M.C., 2001, "Waste Package Project FY-01 Closure Methods Report", Bechtel SAIC Company, LLC, Las Vegas, NV.

Plinski, M.J., 2001, "Waste Package Operations Fabrication Process Report", Bechtel SAIC Company, LLC, Las Vegas, NV.

Prime, M.B., 1999, "Residual stress measurement by the successive extension of a slot: The crack compliance method", Applied Mechanics Reviews, 52, pp. 75-96.

Appendix A

The peening parameters actually employed in the peening of the 3/8 and 1 inch welded plates are summarized in the following table:

Table 4: Laser peening process parameters used

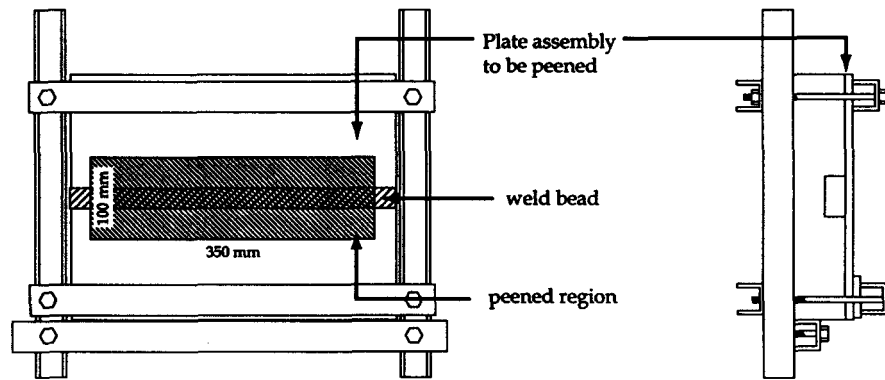
Parameter	Value
Laser pulse energy (at part)	14 J
FWHM (full width half maximum) pulse duration	25 ns
Spot dimension	2.3 by 2.5 mm
Irradiance (power per area)	9.7 GW/cm ²
Spot overlap (between successive spots)	10%
Number of layers	10
Layer overlap (between successive layers)	20%
Ablative layer	Al tape, 2 layers

The plate assemblies laser peened at LLNL had the following identification numbers:

Table 5: Plate identification

Plate thickness (in)	Part Number
3/8	HT XX2213BC E1B
3/8	HT XX2213BC E2B
3/8	HT XX2213BC E3B
1	HT XX2246BG F1B
1	HT XX2246BG F2B

The plates were mounted to an X-Y material handling stage positioned so that the weld bead ran in a horizontal direction. A PC running LabView controlled the planar movement of the stage. The fixturing of a welded plate is shown in the figure below.



Supporting machine structure not shown for clarity

Figure 25: Schematic of the fixturing of the stress mitigation welded coupons

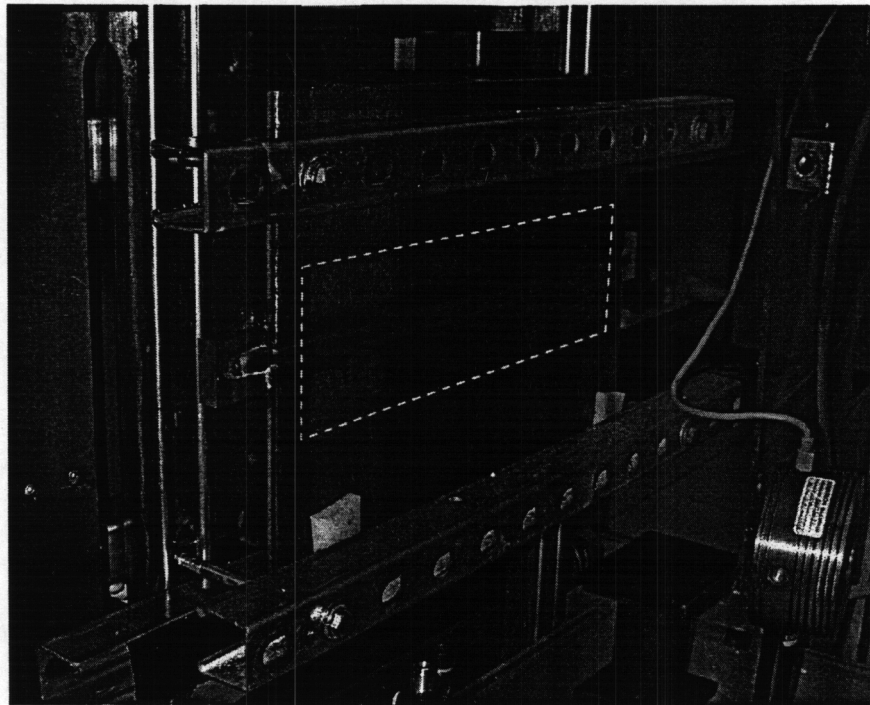


Figure 26: Photograph of the stress mitigation welded coupons; the laser peening is indicated by a dashed rectangle parallel to the weld bead.

Prior to peening, the plate was cleaned with acetone and ethyl alcohol, and dried with a heat gun. Two layers of aluminum tape were applied after the plate was dry. Between layers of peening, the used tape was removed, the surface was re-cleaned, and new tape was applied.

A fixed plexiglass shield was erected to minimize blowback of peening debris towards the delivery lens in the laser system. Additional protection was provided by 'puffing' compressed air across the processing area to clear debris from the beam path between laser shots.

Appendix B

The following journal articles, “The Effects of Process Variations on Residual Stress in Laser Peened Al 7049 T73 Aluminum Alloy” (Mat. Sci. Eng. A, to Appear) and “Cross-Sectional Mapping of Residual Stresses by Measuring the Surface Contour After a Cut” (Trans. Am. Soc. Mech. Eng., 2001) give technical details and experimental applications for the two mechanical release residual stress measurement methods used in this work, the slitting method and the contour method respectively.